JOURNAL OF SOLID STATE CHEMISTRY 103, 458–465 (1993)

Crystal Structure Determination and Physical Properties of the Misfit Compound $(NdS)_{1.18}NbS_2$

A. LAFOND, A. MEERSCHAUT, P. GRESSIER, AND J. ROUXEL

Institut des Matériaux de Nantes, Laboratoire de Chimie des Solides, UMR 110, Université de Nantes, 2, rue de la Houssinière, 44072 Nantes Cedex 03, France

Received July 13, 1992; in revised form September 23, 1992; accepted September 24, 1992

The crystal structure of the new misfit layer compound $(NdS)_{1.18}NbS_2$ has been determined by a composite approach which leads to average structures and their relative arrangement. $(NdS)_{1.18}NbS_2$ is built of $|NdS|$ double layers (approximately a {100} slice of NaCl type) alternating with $|NbS_2|$ sandwiches in which an Nb atom is surrounded by a trigonal prismatic arrangement of S atoms. Both subsystems ($|NdS|$ and $|NbS_2|$) are F centered (orthorhombic space group $Fm2m$). Resistivity measurements (300–5 K) indicate metallic behavior attributed to the presence of an almost filled $4dz^2$ (Nb) band of the $|NbS_2|$ part. The inverse magnetic susceptibility as a function of temperature shows linear variation over the whole temperature range (300–4.2 K). An effective moment of $\mu_{exp} = 3.7\ \mu_B$ is deduced, very close to the theoretical Nd^{3+} free ion value ($\mu_{theor} = 3.62\ \mu_B$). A large magnetic anisotropy is observed, as made evident by the magnetization curves measured at 1.85 K with a magnetic field applied parallel and perpendicular to the crystal plane ((a, b) plane).

Introduction

Niobium and tantalum dichalcogenides show layer structures built with $|XMX|$ slabs where the metal atoms may have a trigonal prismatic coordination ($2H$ form) or an octahedral one ($1T$ form). Very interesting is the fact that exists a polytype with both types of slabs ($4H_b$). Trials to prepare phases with an alternation of trigonal prismatic slabs of NbS_2 and octahedral slabs brought in by another element (TiS_2 slabs for example) have failed (*1*).

However, such a situation, implying a succession, in a given chalcogenide structure, of layers showing two types of coordination for two distinct metallic elements has recently been approached in "MNbS$_3$" phases with M = Sn, Pb, Bi, La, Sm, . . . (*2–5*). The structure of these phases results from a stacking of NbS_2 trigonal prismatic slabs and MS slabs which can be assimilated to a distorted {100} slice of an NaCl arrangement (pseudooctahedral). Both sublattices are characterized by sets of a and b in-plane parameters and a common c periodicity in the direction perpendicular to the slabs. The two b parameters have been found, up to now, to be strictly identical. But the ratio of the a values is irrational. For that reason these compounds are called *misfit layer compounds*. The incommensurability is directly reflected in $(MS)_nNbS_2$ formulations with n values in the 1.08–1.24 range. The value of n has been deduced as follows: the unit cells of the $|MS|$ and $|NbS_2|$ substruc-

0022-4596/93 $5.00

TABLE I

CHEMICAL ANALYSIS ON $(NdS)_{1.18}NbS_2$ CRYSTALS (ATOMIC PERCENTAGES)

	Nd	Nb	S
Experimental	22.7(1.0)	17.7(1.0)	59.6(1.0)
Theoretical	22.0	18.3	59.3

tures contain four and two units; respectively. Thus, in a fixed volume of the crystal, the ratio of units of NbS_2 to units of MS is given by $2V_2/V_1$, where V_1 and V_2 are the volumes of $|MS|$ and $|NbS_2|$ subcells, respectively; the factor of 2 is the ratio of the number of formulas per unit of the two subsystems. For the orthorhombic compound the ratio V_2/V_1 is then equal to a_2/a_1 and $n = 2a_2/a_1$, a_1 and a_2 being the a parameters of the $|MS|$ and $|NbS_2|$ parts, respectively.

A good characterization of each compound is necessary to understand the interesting physical properties that are suggested by preliminary measurements (*6, 7*). Indeed the misfit, i.e., the structural characteristics and chemical formulation changes from one compound to the other. An electronic transfer takes place from the $|MS|$ slab to the $|NbS_2|$ ones. It is quite nonexistant when M = Pb or Sn, but close to one electron when M = La. There is a need to increase the number of well characterized compounds and also to design phases showing new features. We have been able recently to extend the series to "MNb_2S_5" phases presenting two successive $|NbS_2|$ slabs between $|MS|$ layers. Superconducting properties depend on the stacking mode of the $|NbS_2|$ slabs relative to each other.

In the present paper, a neodymium misfit layer compound is presented. Such a compound was prepared to introduce a magnetic layer between conducting $|NbS_2|$ slabs.

Experimental

$(NdS)_{1.18}NbS_2$ was prepared by heating a mixture of Nd_2S_3 and NbS_2 in a 0.6 : 1 ratio at a temperature of 1000°C for 2 weeks in a silica tube sealed under vacuum ($\sim 10^{-2}$ Torr). The initial powders were pressed into pellets to favor reaction and to minimize the contact with the silica tube, which was protected by a thin carbon film. An intermediate crushing and repastillating was done to favor homogenization. Nd_2S_3 was obtained after sulfurizing Nd_2O_3 (gas flow of H_2S/Ar) at 1300–1350°C for 4 hr. NbS_2 was prepared by heating Nb + 2S (slight excess of sulfur) at 850°C for 10 days.

TABLE II

X-RAY POWDER DIFFRACTION PATTERN OF $(NdS)_{1.18}NbS_2$

hlk	type	d_{obs} (Å)	d_{calc} (Å)	I_{obs}
004	c	5.667	5.666	17
111	a	3.958	3.960	18
006	c	3.778	3.777	100
113	a	3.548	3.550	46
115	a	3.0069	3.0083	9
020	c	2.8696	2.8710	24
111	b	2.8589	2.8584	12
008	c	2.8322	2.8328	31
200	a	2.8157	2.8175	31
022	c	2.7802	2.7831	24
202	a	2.7385	2.7343	14
024	c	2.5605	2.5610	8
026	c	2.2855	2.2857	67
0010	c	2.2669	2.2663	19
117	b	2.1451	2.1524	8
119	a	2.1316	2.1343	33
220	a	2.0102	2.0109	32
208	a	1.9987	1.9977	4
222	a	1.9803	1.9800	25
0012	c	1.8890	1.8886	36
311	a	1.7790	1.7797	24
0210	c		1.7789	
131	b	1.6554	1.6550	22
202	b	1.6595	1.6480	26
0212	c	1.5779	1.5778	9
139	a	1.4713	1.4710	9
0016	c	1.4168	1.4164	24

Note. Unit cell parameters least-square refinements have been done for separate |NdS| and $|NbS_2|$ parts. |NdS| part: a_1 = 5.635(1) Å, b_1 = 5.742(1) Å, c_1 = 22.663(3) Å. $|NbS_2|$ part: a_2 = 3.3313(9) Å, b_2 = 5.742(1) Å, c_2 = 22.663(3) Å.

a: |NdS| part, b: $|NbS_2|$ part, c: common.

TABLE III

CRYSTAL DATA AND DETAILS OF REFINEMENTS

⟨|NdS| part⟩
Orthorhombic symmetry, S. G. $Fm2m$ (No. 42), $Z = 8$
Unit cell parameters
$a_1 = 5.635(1)$ Å, $b_1 = 5.7421(7)$ Å, $c_1 = 22.663(3)$ Å
Mo$K\alpha$ radiation (graphite monochromator, $\lambda = 0.71073$ Å) $2° < \theta < 35°$, ω scan mode, $\Delta\omega = 1.10 + 0.35$ tg θ 257 unique reflections ($I > 3\sigma(I)$, excluding $h = 0$) 13 refined parameters
$R = \Sigma (||F_o| - |F_c||)/\Sigma |F_o| = 0.056$
$R_w = [\Sigma w(|F_o| - |F_c|)^2/\Sigma w|F_o|^2]^{1/2} = 0.079$ with $w^{-1}(F^2) = [\sigma^2(I) + (0.04\,F^2)^2/]\,4F^2$
ESD $= [\Sigma w(|F_o| - |F_c|)^2]/(m - n) = 3.065$ with
m = number of observations
n = number of refined parameters
Highest peak in Fourier difference $\pm 1.4\ e^-$ Å^{-3}

⟨$|NbS_2|$ part⟩
Orthorhombic symmetry, S. G. $Fm2m$ (No. 42), $Z = 4$
Unit cell parameters
$a_2 = 3.331(1)$ Å, $b_2 = 5.742(1)$ Å, $c_2 = 22.663(23)$ Å
Same data collection conditions as for the |NdS| part
124 unique reflections ($I > 3\sigma(I)$, $h = 0$ excluded), 10 variables
$R = 0.092$, $R_w = 0.113$ with $w^{-1}(F^2) = [\sigma^2(I) + (0.04\,F^2)^2/]4F^2$
ESD = 3.607
Highest peak in Fourier difference $\pm\ 0.7\ e^-$ Å^{-3}

⟨Common part: $b' = 2.871$ Å, $c' = 11.331$ Å⟩
72 unique reflections ($I > 2\sigma(I)$), $h = 0$ only, 8 variables
$R = 0.072$, $R_w = 0.117$ with $w^{-1}(F^2) = [\sigma^2(I) + (0.04\,F^2)^2/]4F^2$
ESD = 5.41
Highest peak in Fourier difference $\pm\ 0.8\ e^-$ Å^{-3}

TABLE IV

POSITIONAL PARAMETERS AND THEIR ESTIMATED STANDARD DEVIATIONS; B_{eq} (Å^2) AND OCCUPANCY FACTORS

⟨|NdS| part⟩

	x	y	z	B_{eq}(Å^2)
Nd	0	0	0.32505(6)	1.72(2)
S(1)	0	0.014(1)	0.2002(2)	0.93(8)

	U_{11}	U_{22}	U_{33}	U_{23}	(×10^4)
Nd	217(5)	226(5)	210(44)	−67(14)	
S(1)	139(19)	32(19)	182(20)	12(27)	

⟨$|NbS_2|$ part⟩

	x	y	z	B_{eq} (Å)
Nb	0	0	0	0.45(4)
S(2)	0	0.332(2)	0.0674(5)	1.8(2)

	U_{11}	U_{22}	U_{33}	U_{23}	(×10^4)
Nb	38(10)	72(8)	62(11)	—	
S(2)	345(64)	190(38)	157(45)	−37(32)	

⟨Common part: $b = 2.871$ Å, $c = 11.331$ Å⟩

	x	y	z	Mult	B_{iso}(Å^2)
Nd	—	0	0.6512(4)	0.58	1.17(7)
S(1)	—	0.0283(-)	0.401(-)	0.58	1.3(4)
Nb	—	−0.147(2)	0	0.5	0.01(5)
S(2)	—	0.5175(-)	0.1349(-)	1	−0.2(1)

Single platelet-shaped crystals of $(NdS)_{1.18}NbS_2$ are formed in the low-temperature side of the tube (gradient of about 50°C, between 950 and 1000°C) by using iodine as a transport agent.

Chemical analysis was carried out with an electron microprobe (TRACOR model, dispersive energy). Results are given in Table I where they are compared to the theoretical values calculated from the $(NdS)_{1.18}NbS_2$ formulation.

The X-ray powder diffraction pattern was obtained from a cylindrical position sensitive detector (INEL apparatus) with a strictly monochromatized Cu$K\alpha_1$ radiation ($\lambda = 1.540598$ Å). Lattice parameters of both |NdS| and $|NbS_2|$ subparts were refined by a least-squares method (see Table II).

Structure Determination

A single crystal of $(NdS)_{1.18}NbS_2$ having the appropriate dimensions of $0.17 \times 0.1 \times 0.03$ mm^3 was mounted on an Enraf–Nonius CAD4 diffractometer using Mo$K\alpha$ graphite monochromatized radiation. Preliminary

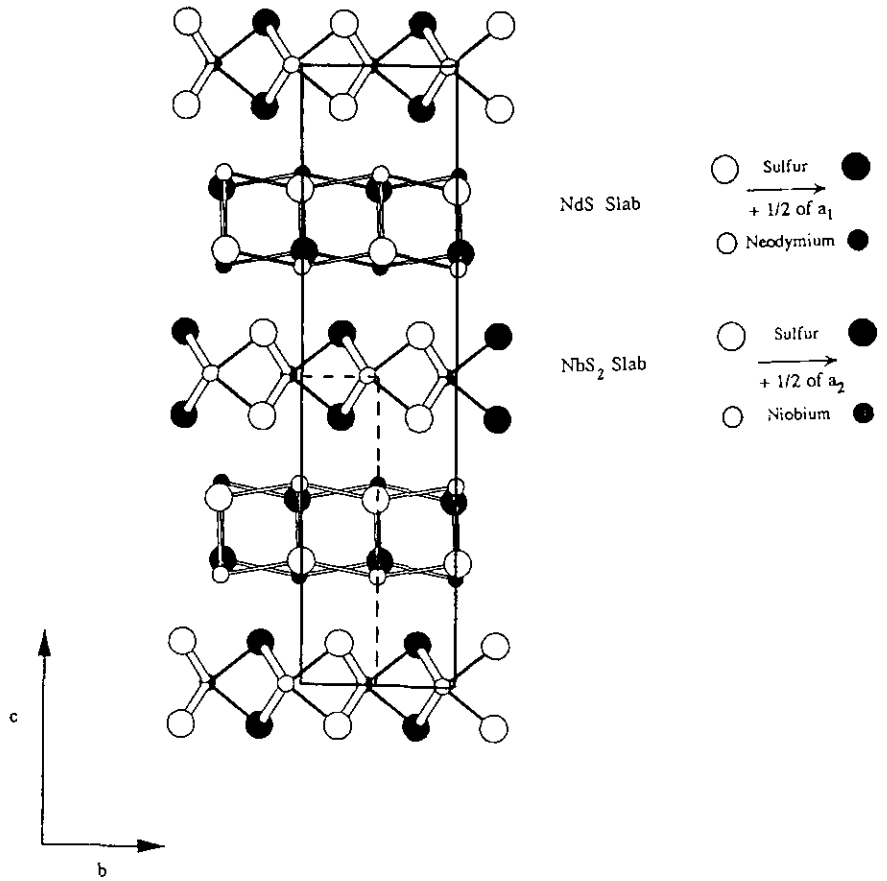

FIG. 1. The structure of $(NdS)_{1.18}NbS_2$ projected along the [100] axis. The small unit cell used for common part refinement is drawn with dotted lines.

studies by Weissenberg and Buerger X-ray techniques revealed that the reflections can be indexed using two *F* centered orthorhombic unit cells for the |NdS| and $|NbS_2|$ sublattices. Because the ratio of the *a*-periodicities of the two sublattices is irrational (a_1/a_2 = 1.691) it is not possible to choose a larger unit cell giving a description of the whole structure and we are left with the two subparts given in Table II. The structure determination was therefore divided into three parts:

(i) The |NdS| part excluding common reflections with the $|NbS_2|$ one; thus, reflections for which $h = 0$ were excluded.

(ii) The $|NbS_2|$ part (h = 0 excluded for the same reason).

(iii) The common part using *okl* reflections only, to adjust the relative *y* and *z* positions of both structure parts in the complete structure. Due to incommensurability along the *a* axis it is not possible to fix *x* coordinates.

Besides these main reflections, satellite reflections originating from the mutual modulations of both sublattices are expected.

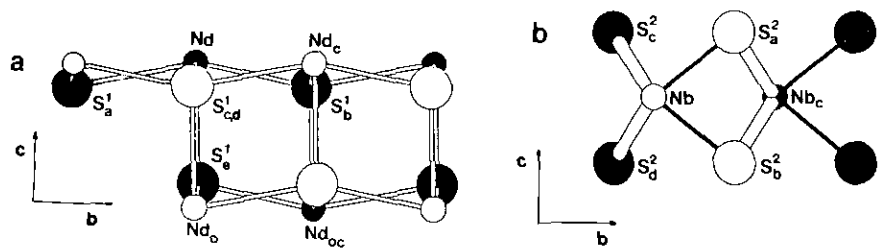

FIG. 2. Detail of |NdS| part (a) and |NbS2| part (b) projected along [100] axis.

However, in the composite approach those reflections are ignored. Therefore only average structures can be determined; i.e., the mutual modulation of the two subsystems |NdS| and $|NbS_2|$ is neglected.

Data collection conditions are summarized in Table III. Intensities were corrected for Lorentz and polarization effects. We also used the DIFABS program as recommended by Walker and Stuart (*8*) to correct intensities for absorption effects. That correction was done each time on each separate part. SDP Enraf–Nonius programs are used.

(a) The |NdS| Part

Systematic extinction conditions are observed for $h + k$, $k + l$, and $h + l = 2n + 1$, indicating an F centered type. Refinement was conducted in the Fm2m (no. 42) space group with atoms (Nd and S(1)) on site 8(c): $o, y, z; o, y, \bar{z}$. The y coordinate of Nd was arbitrarily set equal to zero. Refinements on F by full-matrix least squares converged at $R = 0.056$, $R_w = 0.079$, ESD = 3.065 for 257 unique reflections ($I > 3\sigma(I)$) and 13 variables, using weighting scheme No. 1 ($w^{-1} = (\sigma^2(I) + (pF^2)^2)/4F^2$ with $p = 0.04$). Reflections with the weakest intensities ($F_o < 7.0$, $F_o^{max} = 70.7$) were disregarded, as well as five "bad" reflections (asymmetric background $\rightarrow F_o < F_c$). Rejection of the weakest reflections can be justified by the observation of diffuse lines on photographic film indicating a certain amount of disorder (probably a misorientation of blocks |NdS|/$|NbS_2|$; see Kuypers *et al.* (*9*) for a detailed discussion). Table IVa summarizes the final fractional coordinates and the thermal vibrational parameters.

TABLE V

MAIN INTERATOMIC DISTANCES (Å)

|NdS| part		$|NbS_2|$ part	
Nd–S(1)$_a$	2.85(1)	Nb–2 × S(2)$_a$	2.44(1)
–S(1)$_b$	3.01(1)	–2 × S(2)$_b$	2.44(1)
–S(1)$_c$	2.876(1)	–S(2)$_c$	2.457(9)
–S(1)$_d$	2.876(1)	–S(2)$_d$	2.457(9)
–S(1)$_e$	2.831(4)	Nb–Nb$_c$	3.319(2)
(Nd–S(1))av	2.89		
Nd–2 × Nd$_c$	4.023(1)		
Nd–2 × Nd$_o$	4.451(1)		
Nd–Nd$_{oc}$	4.417(1)		

(b) The $|NbS_2|$ Part

The "NbS_2 reflections" are only present for $h + k$, $k + l$, and $h + l = 2n$, indicating an F centered lattice. Refinement was conducted in the *Fm2m* (No. 42) space group with Nb atoms on site 4(a): o, y, o and S(2) atoms on site 8(c): $o, y, z; o, y, \bar{z}$. One of the y coordinates may be chosen arbitrarily; thus, $y = 0$ was chosen for Nb. Refinements converged at $R = 0.092$ and $R_w = 0.112$ for 128 unique reflections ($I > 3\sigma(I)$) and 10 variables using weighting scheme No. 1 (as above). Reflections with the weakest intensities ($F_o < 6.0$, $F_o^{max} = 50.8$) were disre-

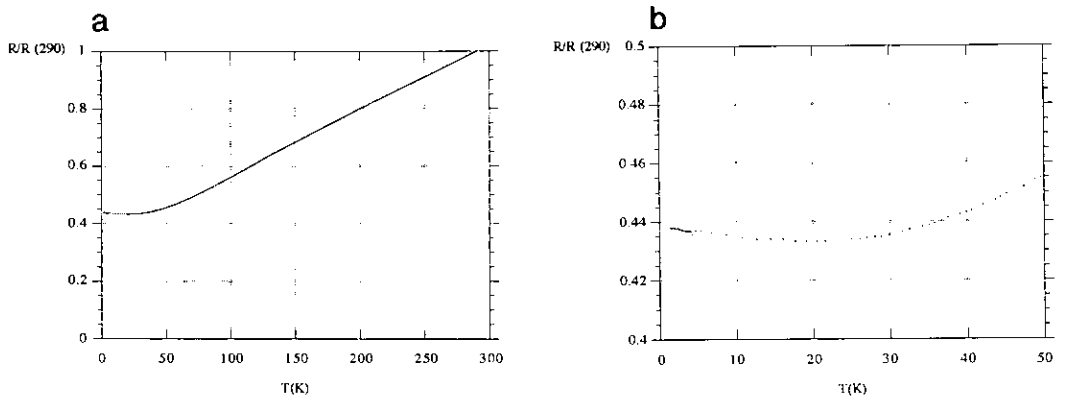

FIG. 3. The variation of $R/R(290)$ ratio versus T in the range 1.4–290 K (a) and 1.4–50 K (b) for $(NdS)_{1.18}NbS_2$.

garded for the same reason as above. Final fractional coordinates and anisotropic thermal parameters (Us) are given in Table IVb.

(c) The Common Part

The common projection was deduced from the *okl* reflections common to both |NdS| and $|NbS_2|$ sublattices; since the *okl* reflections are only present for $k = 2n$ and $l = 2n$, a smaller unit cell can be chosen for the refinement, resulting in a unit cell with $b' = b/2 = 2.871$ Å and $c' = c/2 = 11.331$ Å. Refinements were performed in space group $P11m$ (No. 3 of the 17 two-dimensional space groups). Atomic coordinates within each sublattice were constrained in order to preserve the same values for Δy and Δz between atoms within the respective sublattice as refined in their separate parts. Only the z coordinate of Nd and the y coordinate of Nb were refined to result in the relative $|NdS|/|NbS_2|$ arrangement in the plane projection.

The site occupancy factors of Nd and S(1) atoms (|NdS| part) were kept equal and refined relative to the contribution of the $|NbS_2|$ part. Refinements made step by step led to minimum R factors for the ratio $|NdS|/|NbS_2|$ equal to 0.58/1. This ratio is almost identical to the one deduced from the a parameter values ($n = 2 \times a_2/a_1 = 1.18 \rightarrow$ a ratio $|NdS|/|NbS_2| = 0.59/1$ taking into account the number of formula units per unit cell of the two subsystems).

Refinement by full-matrix least squares using 72 unique *okl* reflections ($I > 2\,\sigma(I)$) converged to $R = 0.072$ and $R_w = 0.117$ (weighting scheme No. 1 as discussed above). Coordinates and isotropic thermal parameters are reported in Table IVc.

Discussion of the Structure

A projection of the complete structure onto the (b, c) plane is shown in Fig. 1; the small unit cell used for common part refinement is drawn with dotted lines.

The |NdS| part is made of a double plane of Nd–S atoms; the midplane of this part is a mirror plane at $z = \frac{1}{2}$. The Nd atoms protrude from the planes of sulfur as already found in the other $|MS|$ parts of the "MTS_3" compounds (*3*). Each Nd atom is coordinated to five S atoms distributed over a slightly distorted square pyramidal arrangement (see Fig. 2a) with Nd–S distances as indicated in Table V. These Nd–S(1) distances agree well with that found in the NdS binary

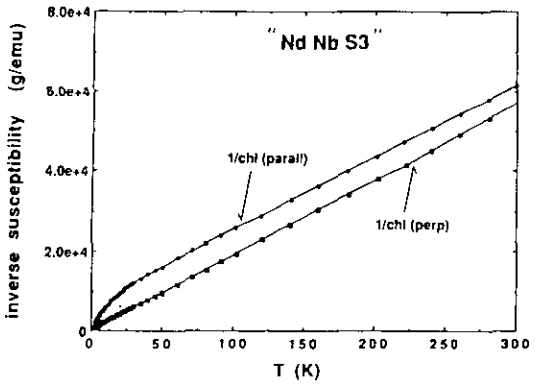

FIG. 4. Inverse susceptibility of $(NdS)_{1.18}NbS_2$ single crystals oriented parallel and perpendicular to the applied field.

compound (2.847 Å) for which a similar structural arrangement is observed (*10*).

The $|NbS_2|$ part is built of edge-sharing trigonal prisms (see Fig. 2b) as in 2H–NbS_2. Niobium atoms are located in the mirror planes at $z = 0$. The Nb–S(2) distances are summarized in Table V. The six S atoms surrounding the Nb atom are at the same distance of Nb (~2.45 Å) as noticed for parent "$MNbS_3$" compounds.

Along the *c* direction, alternate |NdS| and $|NbS_2|$ layers are stacked such as the Nd atoms are lying in between rows (‖ to *a* axis) of $|NbS_2|$ sulfurs. Thus the Nd atoms are not only coordinated to the five S(1) atoms of the |NdS| part but also to S(2) atoms of the $|NbS_2|$ part. Incommensurability along the *a* axis and the composite approach make it impossible to calculate the Nd–S(2) distances. However, the limits of these distances can be calculated assuming Δx values (between Nd and S(2)) ranging from 0 to $a_2/2$; this leads to a 2.79 Å < Nd–S(2) < 3.25 Å.

Transport and Magnetic Properties

Resistivity measurements were performed on a single crystal (platelet-shape) with the four contact technique. Figure 3a shows the variation of $R/R_{290\,K}$ as a function of temperature between 1.4–290 K. A typical metallic behavior is observed above 50 K. At lower temperature ($T < 20$ K), a slight increase of the resistance is occurring (see Fig. 3b). No superconducting transition was observed at lowest temperatures. This was also the case for the Gd derivative. On the contrary, $(LnS)_nNbS_2$ compounds (with La, Ce, and Sm) are found to be superconductors (*11*). This is also the case with all nonmagnetic $(MS)_nNbS_2$ (M = Sn, Pb, Bi) (*3*).

This leads to a few remarks:

—There is no simple relationship between the presence of magnetic ions (within the $|MS|$ layer) and the occurrence of superconductivity. The influence of the magnitude of magnetic moment, up to now, has been difficult to ascertain due to the number of unstudied cases (e.g., Pr, Er, Dy, . . . derivatives).

—Also, the magnetic order is not a criterion to explain the absence of superconductivity. Indeed, both Ce and Gd derivatives exhibit an antiferromagnetic order but the former is a superconductor while the latter is not.

—The charge transfer from $|MS|$ to $|NbS_2|$, being weak for Sn, Pb, and Bi and stronger for Ln, does not seem to be a pre-

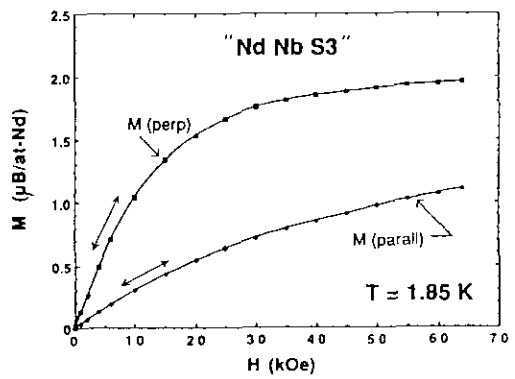

FIG. 5. Magnetization at 1.85 K of oriented single crystals of $(NdS)_{1.18}NbS_2$.

dominant factor explaining the occurrence of a superconducting transition. The presence of $|NbS_2|$ is undoubtedly at the origin of the superconductivity. These slabs are well isolated. The separation from external magnetic layers is much better achieved than in M_xNbS_2 pseudointercalation compounds (*11*). Weak local fields such as the one generated by Ce^{3+} ions are not able to destroy superconductivity.

The magnetic susceptibility as a function of temperature was measured along two directions: H perpendicular or parallel to the a–b plane. A linear variation of χ^{-1} versus T was observed in the whole temperature range when the field was applied perpendicular to the crystal planes (Fig. 4). The same slope was observed for the other direction above 50 K. An effective moment of 3.7 μ_B is obtained, close to the theoretical Nd^{3+} free ion value (μ_{theor} = 3.62 μ_B). A large magnetic anisotropy is observed as evidenced by the magnetization curves measured at 1.85 K (Fig. 5). The curve saturates to $2\mu_B$/Nd-atom at about 60 kOe along the easy axis of magnetization (H perpendicular to the a–b plane and parallel to the c axis), while it reaches only half of that value along the planes. Neither hysteresis nor remanent magnetization was observed. A more detailed magnetic study is to be found in another paper (*7*, *12*) and for the $(NdS)_{1.17}TaS_2$ compound (*13*).

Acknowledgments

The authors thank Dr. Monceau and Dr. Chen (CRTBT CNRS Grenoble) for their contributions to resistivity measurements.

References

1. J. Rouxel, A. Meerschaut, and P. Palvadeau, unpublished results.
2. A. Meerschaut, P. Rabu, and J. Rouxel, *J. Solid State Chem.* **78,** 35–45 (1989).
3. A. Meetsma, G. A. Wiegers, R. J. Haange, and J. L. de Boer, *Acta Crystallogr. Sect. A* **45,** 285–291 (1989).
4. G. A. Wiegers, A. Meetsma, R. J. Haange, S. Van Smaalen, J. L. de Boer, A. Meerschaut, P. Rabu, and J. Rouxel, *Acta Crystallogr. Sect. B* **6,** 324–332 (1990).
5. A. Meerschaut, C. Auriel, A. Lafond, C. Deudon, P. Gressier, and J. Rouxel, *Eur. J. Solid State Inorg. Chem.* **28,** 581–595 (1991).
6. G. A. Wiegers, A. Meetsma, R. J. Haange, and J. L. de Boer, *Solid State Ionics* **32/33,** 183–191 (1989).
7. O. Pena, P. Rabu, and A. Meerschaut, *J. Phys. Condensed Matter* **3,** 9929 (1991).
8. N. Walker and D. Stuart, *Acta Crystallogr. Sect. A* **39,** 159 (1983).
9. S. Kuypers, J. van Landuyt, and S. Amelinckx, *J. Solid State Chem.* **86,** 212 (1990).
10. A. Iandelli, *Gazz. Chim. Ital.* **85,** 881–887 (1955).
11. V. M. Vandenberg-Voorhoeve, "Physics and Chemistry of Materials with Layered Structures" (P. A. Lee, Ed.), Vol. 4, Reidel, Dordrecht (1976).
12. P. Rabu, Thesis, University of Nantes (1990).
13. K. Suzuki, T. Enoki, and K. Imaeda, *Solid State Commun.* **78(2),** 73–77 (1991).